

Supporting Information for

# **Multifunctional self-priming hairpin probe-based isothermal nucleic acid amplification and its applications for COVID-19 diagnosis**

Hansol Kim<sup>1,2</sup>, Seoyoung Lee<sup>1</sup>, Yong Ju<sup>1</sup>, Hyoyong Kim<sup>1</sup>, Hyowon Jang<sup>1,2</sup>, Yeonkyung Park<sup>1,2</sup>, Sang Mo Lee<sup>1</sup>, Dongeun Yong<sup>3</sup>, Taejoon Kang<sup>2,4,\*</sup> and Hyun Gyu Park<sup>1,\*</sup>

<sup>1</sup>Department of Chemical and Biomolecular Engineering (BK 21 four), Korea Advanced Institute of Science and Technology (KAIST), 291 Daehak-ro, Yuseong-gu, Daejeon 34141, Republic of Korea

<sup>2</sup>Bionanotechnology Research Center, Korea Research Institute of Bioscience and Biotechnology (KRIBB), 125 Gwahak-ro, Yuseong-gu, Daejeon 34141, Republic of Korea

<sup>3</sup>Department of Laboratory Medicine and Research Institute of Bacterial Resistance, Yonsei University College of Medicine, 50-1 Yonsei-ro, Seodaemun-gu, Seoul 03722, Republic of Korea

<sup>4</sup>School of Pharmacy, Sungkyunkwan University, 2066 Seobu-ro, Jangan-gu, Suwon, Gyeonggi-do 16419, Republic of Korea

\*To whom correspondence should be addressed.

E-mail: hgpark@kaist.ac.kr (H. G. Park); Phone: +82-42-350-3932; Fax: +82-42-350-3910

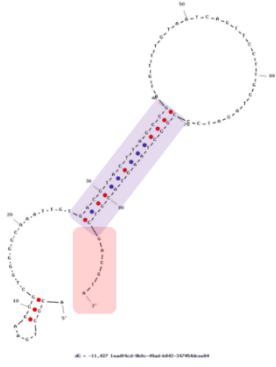
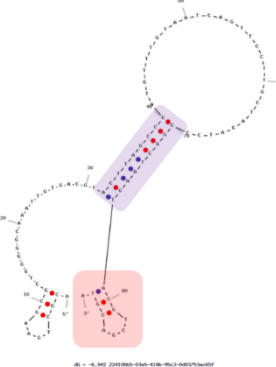
E-mail: kangtaejoon@kribb.re.kr (T. Kang); Phone: +82-42-879-8453

**Table S1.** Oligonucleotide sequences used in this work.

Oligonucleotide	Sequence (5' → 3') <sup>(a)-(e)</sup>
Target RNA (SARS-CoV-2 N RNA; N60)	aag gaa cug auu aca aac auu ggc cgc aaa uug cac aaU uug ccc cca gcg cuu cag cgu
N20	aag gaa cug auu aca aac au
N26	aca auu ugc ccc cag cgc uuc agc gu
SARS-CoV-2 E RNA	gcu uuc gug gua uuc uug cua guu aca cua gcc auc cuu acu gcg cuu cga uug ugu gcg
RSV RNA-1	gug auu caa caa uga cca auu aua uga auc aaU uau cug aaU uac uug gau uug auc uua auc cau aaa uua
RSV RNA-2	aga auu gca guu gcu cau gca aag cac acc ggc aac caa caa ucg agc cag aag aga acu
H3N2 RNA	cuc aag cau cag gaa gaa uca cag ucu cua cca aaa gaa gcc aac aaa cu
ORF1ab target sequence <sup>(f)</sup>	ggg uga ugc gua uua uga cau ggu ugg aua ugg uug aua cua guu ugu cug guu uua agc
MSH (=MSH <sub>6</sub> )	<u>ACG CTG AAG CGC TGG GGG CAA ATT GTG ACG TAC TTA GCC</u> <u>GAT GTT TGT AAT CAG TTC CTT GCT AGA TCC CGG CTA AGT</u> <b>ACG TCG ACG TA</b>
MSH <sub>4</sub>	<u>ACG CTG AAG CGC TGG GGG CAA ATT GTG ACG TAC TTA GCC</u> <u>GAT GTT TGT AAT CAG TTC CTT GCT AGA TCC CGG CTA AGT</u> <b>ACG TCG ACG</b>
MSH <sub>5</sub>	<u>ACG CTG AAG CGC TGG GGG CAA ATT GTG ACG TAC TTA GCC</u> <u>GAT GTT TGT AAT CAG TTC CTT GCT AGA TCC CGG CTA AGT</u> <b>ACG TCG ACG T</b>
MSH <sub>7</sub>	<u>ACG CTG AAG CGC TGG GGG CAA ATT GTG ACG TAC TTA GCC</u> <u>GAT GTT TGT AAT CAG TTC CTT GCT AGA TCC CGG CTA AGT</u> <b>ACG TCG ACG TAC</b>
No tail hairpin	<u>ACG CTG AAG CGC TGG GGG CAA ATT GTG ACG TAC TTA GCC</u> <u>GAT GTT TGT AAT CAG TTC CTT GCT AGA TCC CGG CTA AGT</u> <b>ACG TC</b>
Random tail hairpin	<u>ACG CTG AAG CGC TGG GGG CAA ATT GTG ACG TAC TTA GCC</u> <u>GAT GTT TGT AAT CAG TTC CTT GCT AGA TCC CGG CTA AGT</u> <b>ACG TCT TAT TT</b>
Trigger	AAG GAA CTG ATT ACA AAC ATC GGC TAA GTA CGT CAC AAT TTG CCC CCA GCG CTT CAG CGT
MSH-ORF1ab	<u>GCT TAA AAC CAG ACA AAC TAG TAT CAG ACG TAC TTA GCC</u> <u>GTG TCA TAA TAC GCA TCA CCC GCT AGA TCC CGG CTA AGT</u> <b>ACG TCG ACG TA</b>

- (a) RNA and DNA sequences are represented as lowercase and uppercase letters, respectively.  
(b) Sequences written in blue represent target recognition regions.  
(c) Sequences written in red represent self-priming tail regions.  
(d) Underlined sequences represent stem sequences of MSH.  
(e) The bold characters indicate the recognition sequences of Nt.AlwI.  
(f) Although the 60 nucleotide ORF1ab RNA sequence was not used in the actual experiments, it was included in the manuscript to help the reader understand the target sequence under investigation. This inclusion was intended to provide clarity and context rather than to represent the experimental material used in the study.

**Figure S1.** The secondary structures,  $\Delta G$  of hairpin formation, and melting temperatures ( $T_m$ ) of MSH probe predicted by OligoAnalyzer 3.1 (Integrated DNA Technologies, Inc).

	Structure A	Structure A'
Structure Image		
$\Delta G$ (kcal/mole)	-11.44	-6.95
$T_m$ ( $^{\circ}\text{C}$ )	62.2	54.2

**Figure S2.** NUPACK analysis of the MSH probe with varied RNA target lengths. (a-c) Estimated structures of the MSH probe in interaction with three different RNA targets: (a) N60 RNA, (b) N20 RNA, and (c) N26 RNA. N20 and N26 are complementary to the loop and 5' overhang of the MSH probe, respectively. The analysis parameters were set at a 100 nM concentration for both the MSH probe and the RNA targets, employing DNA-type settings at a consistent temperature of 37 °C.

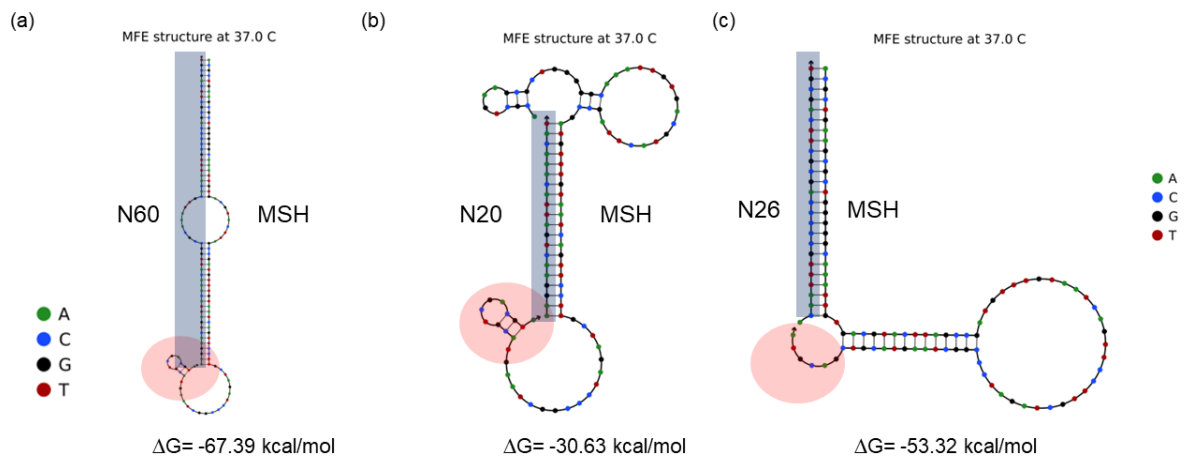


**Figure S3.** Real-time fluorescence curves obtained from the operation of the MSH reaction by employing differently designed self-priming hairpins: (a) Self-priming hairpin (MSH), (b) no tail hairpin, and (c) random tail hairpin. The final concentrations of target RNA, hairpins, KF, and Nt.AlwI are 5 nM, 50 nM, 0.125 U/ $\mu$ L, and 0.4 U/ $\mu$ L, respectively.

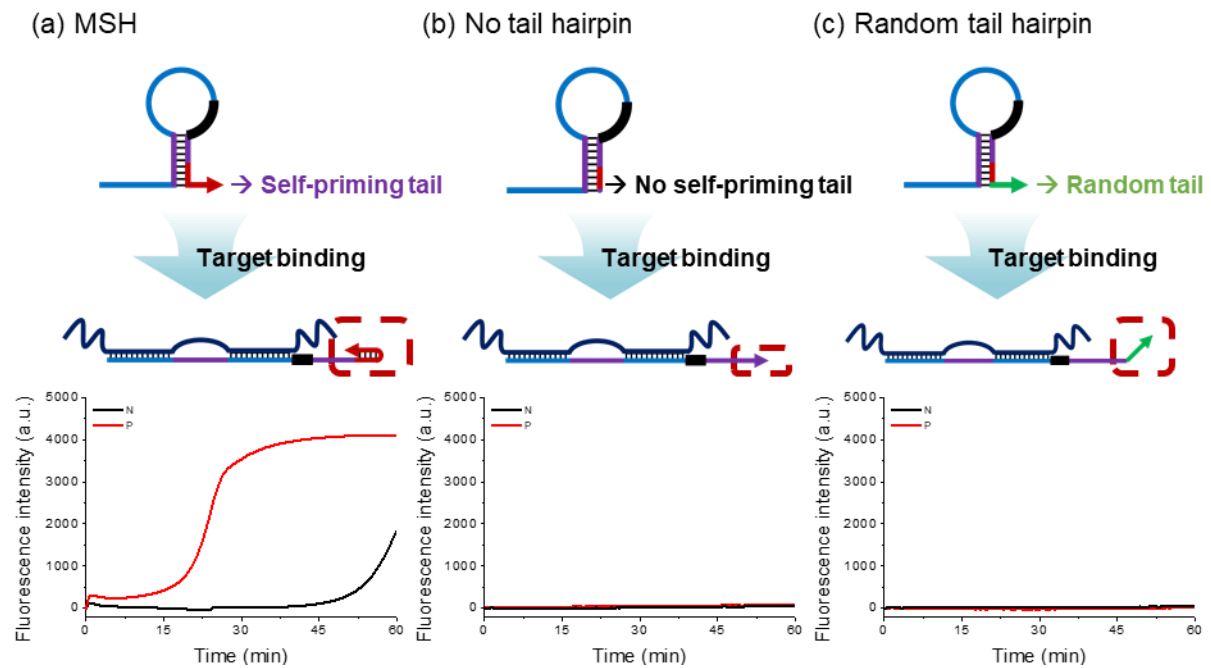


**Figure S4.** Melting curve analysis for the reaction components and products obtained after 10 min reaction at 37 °C. (a) MSH probe + trigger, (b) MSH probe + target RNA + KF, and (c) 1: MSH probe + KF + Nt.AlwI, 2: MSH probe + target RNA + KF + Nt.AlwI. The final concentrations of MSH probe, target RNA, trigger, KF, and Nt.AlwI are 100 nM, 100 nM, 0.125 U/ $\mu$ L, and 0.4 U/ $\mu$ L, respectively. The temperature was increased from 37 to 95 °C. The first negative derivative plot  $[-d(\text{RFU})/dT]$  was used to determine the melting temperature.

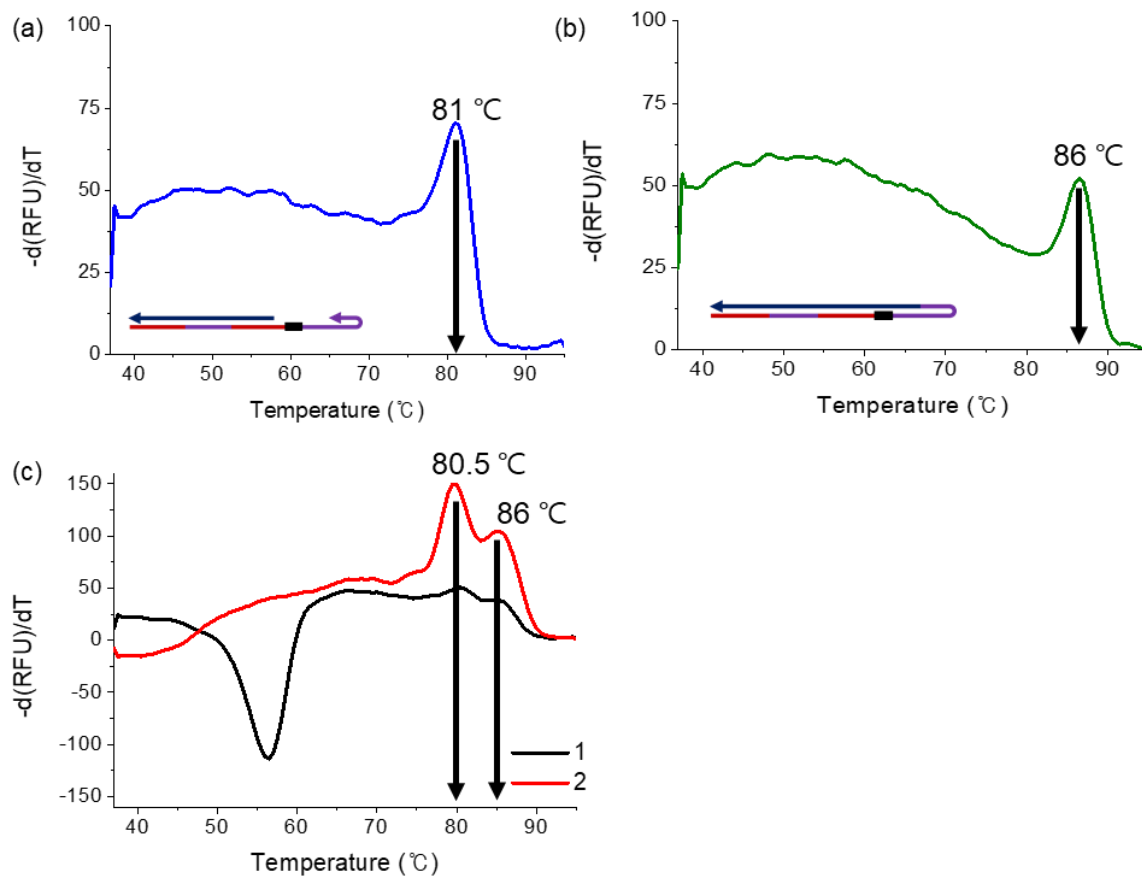


**Figure S5.** Optimization of the tail length. The real-time fluorescence curves were obtained from the MSH reaction for the samples without target RNA (black curves) and with target RNA (red curves). The tail lengths of MSH probe are (a) 4 mer, (b) 5 mer, (c) 6 mer, and (d) 7 mer. The final concentrations of target RNA, MSH probe, and Nt.AlwI are 5 nM, 50 nM, 0.125 U/ $\mu$ L, and 0.25 U/ $\mu$ L, respectively.

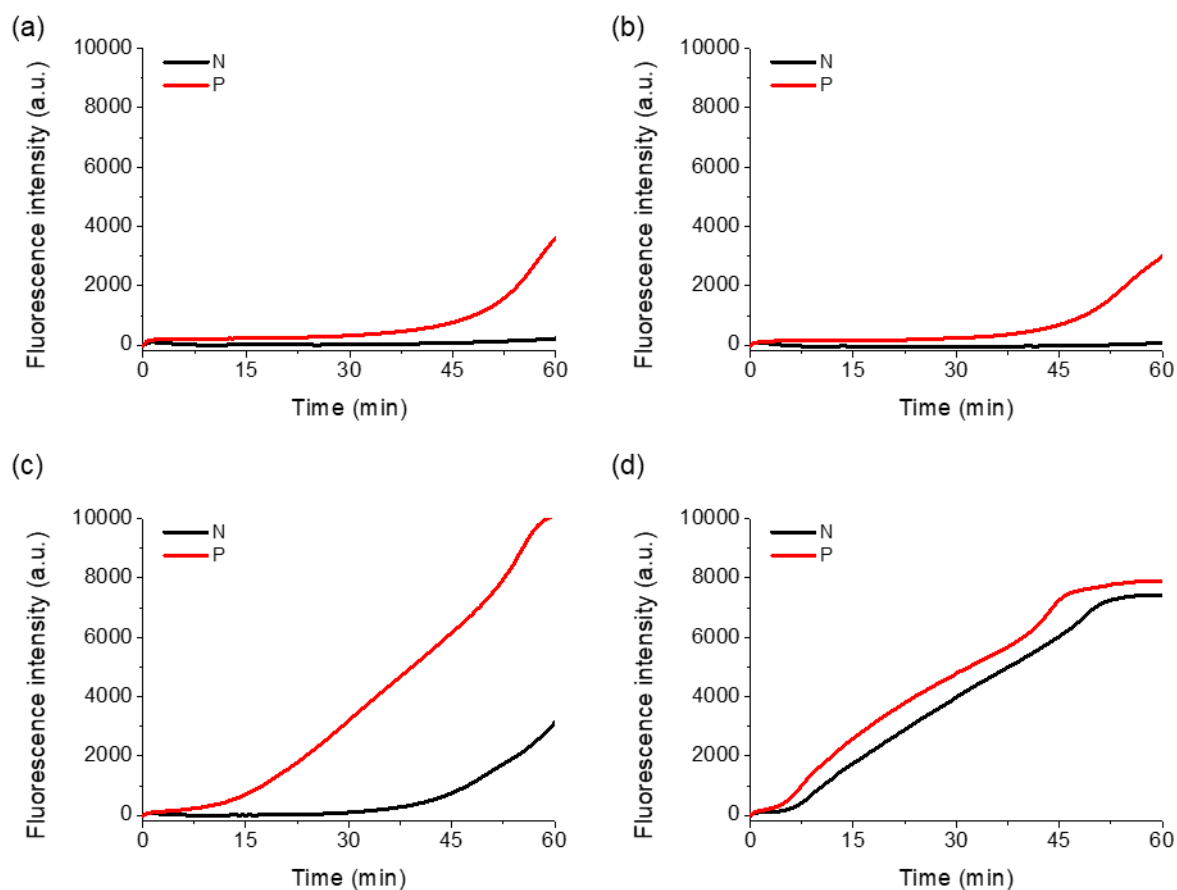


**Figure S6.** Optimization of the MSH probe concentration. The real-time fluorescence curves were obtained from the MSH reaction for the samples without target RNA (black curves) and with target RNA (red curves). The concentrations of MSH probe are (a) 10 nM, (b) 25 nM, (c) 50 nM, and (d) 100 nM. The final concentrations of target RNA, KF, and Nt.AlwI are 5 nM, 0.125 U/ $\mu$ L, and 0.2 U/ $\mu$ L, respectively.

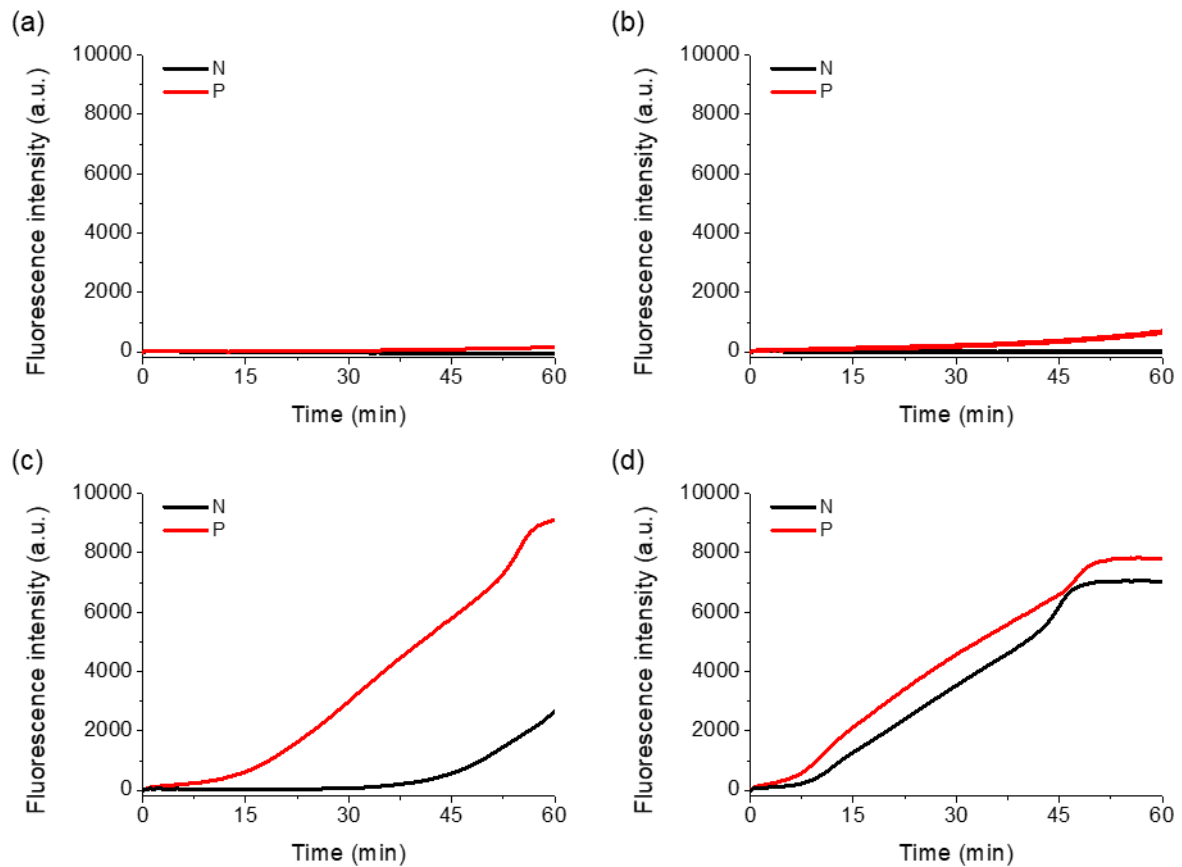




**Figure S7.** Optimization of nicking endonuclease concentration. The real-time fluorescence curves were obtained from the MSH reaction for the samples without target RNA (black curves) and with target RNA (red curves). The concentrations of Nt.AlwI nicking endonuclease are (a) 0.05 U/ $\mu$ L, (b) 0.1 U/ $\mu$ L, (c) 0.2 U/ $\mu$ L, and (d) 0.3 U/ $\mu$ L. The final concentrations of target RNA, MSH probe, and KF are 5 nM, 50 nM, and 0.125 U/ $\mu$ L, respectively.

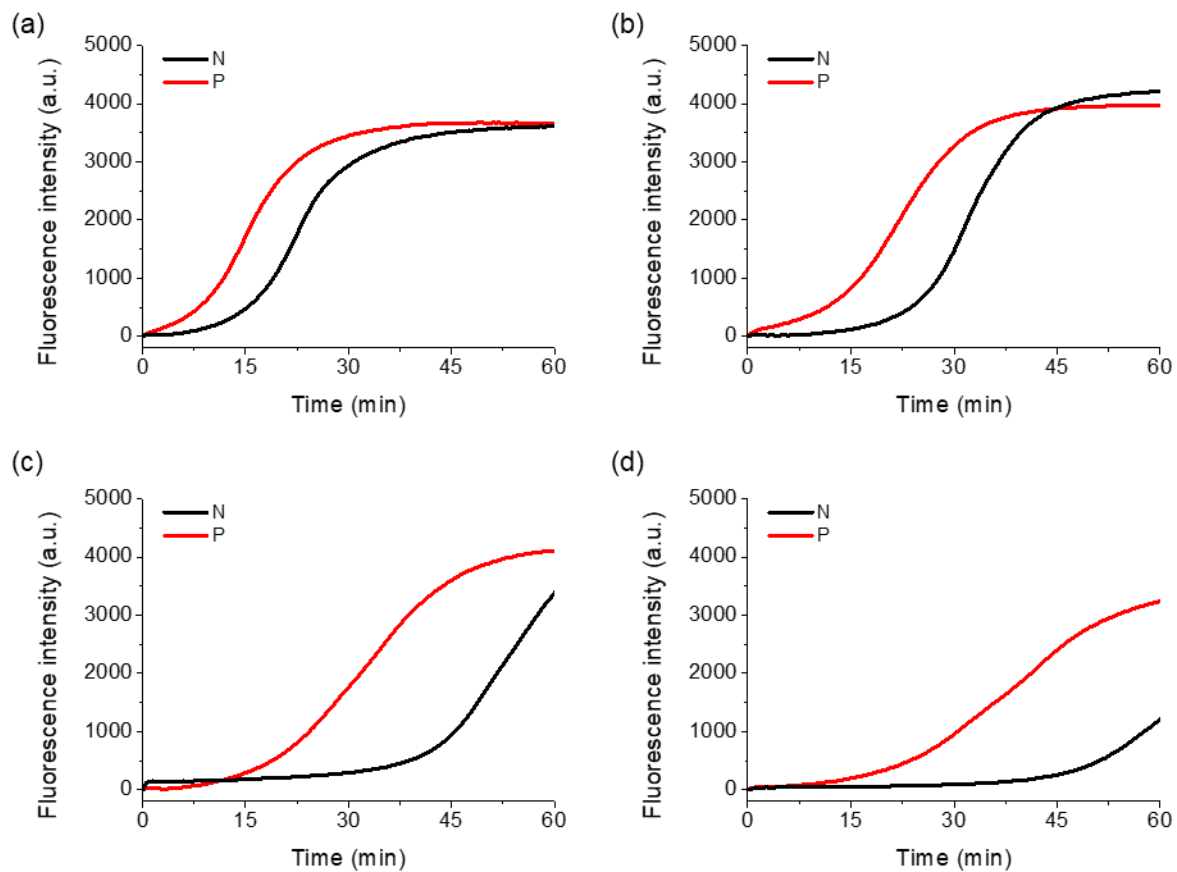


**Figure S8.** Optimization of Klenow DNA Polymerase (exo-) (KF) concentration. The real-time fluorescence curves were obtained from the MSH reaction for the samples without target RNA (black curves) and with target RNA (red curves). The amounts of KF are (a) 0.075 U/ $\mu$ L, (b) 0.1 U/ $\mu$ L, (c) 0.125 U/ $\mu$ L, and (d) 0.175 U/ $\mu$ L. The final concentrations of target RNA, MSH probe, and Nt.AlwI are 5 nM, 50 nM, and 0.2 U/ $\mu$ L, respectively.

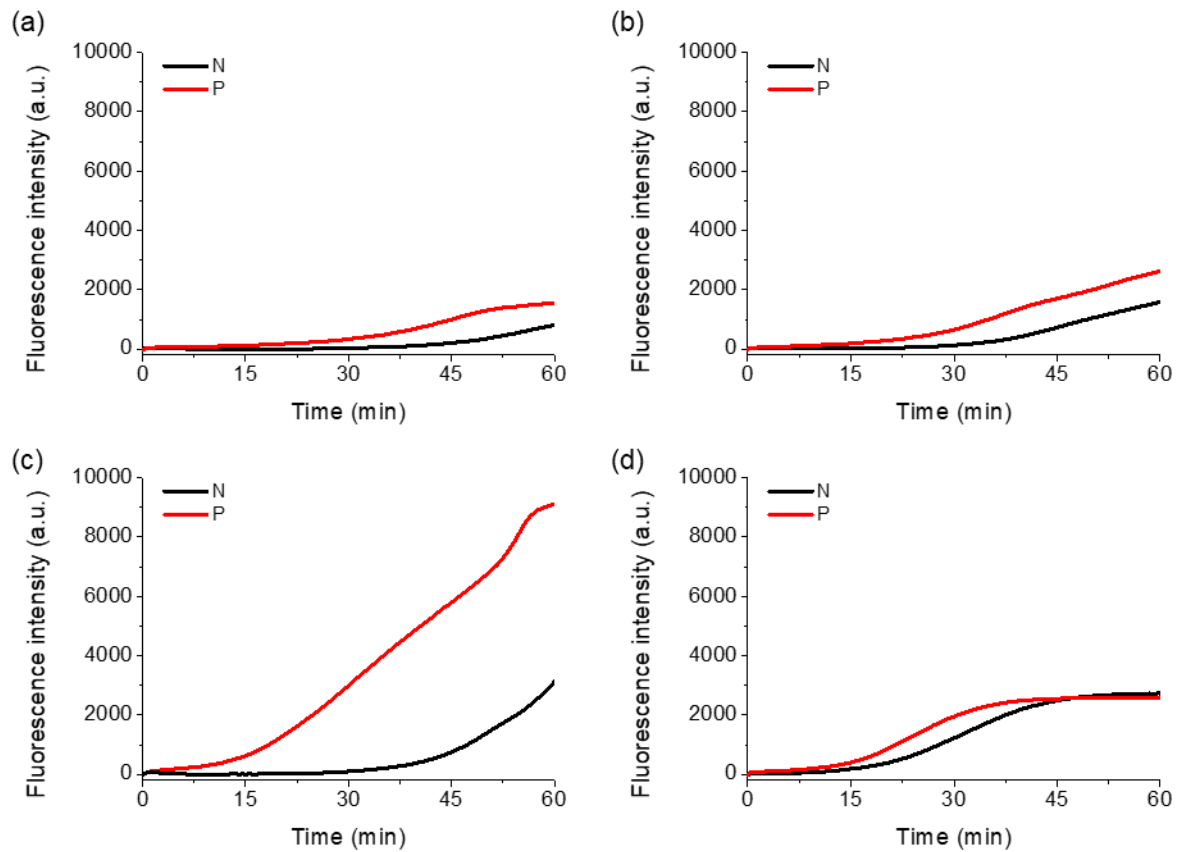


**Figure S9.** The effects of reaction temperature on the MSH reaction. The real-time fluorescence curves were obtained from the MSH reaction for the samples without target RNA (black curves) and with target RNA (red curves). The reaction temperatures are (a) 44 °C, (b) 40 °C, (c) 37 °C, and (d) 33 °C. The final concentrations of target RNA, MSH probe, Nt.AlwI, and KF are 5 nM, 50 nM, 0.125 U/ $\mu$ L, and 0.2 U/ $\mu$ L, respectively.

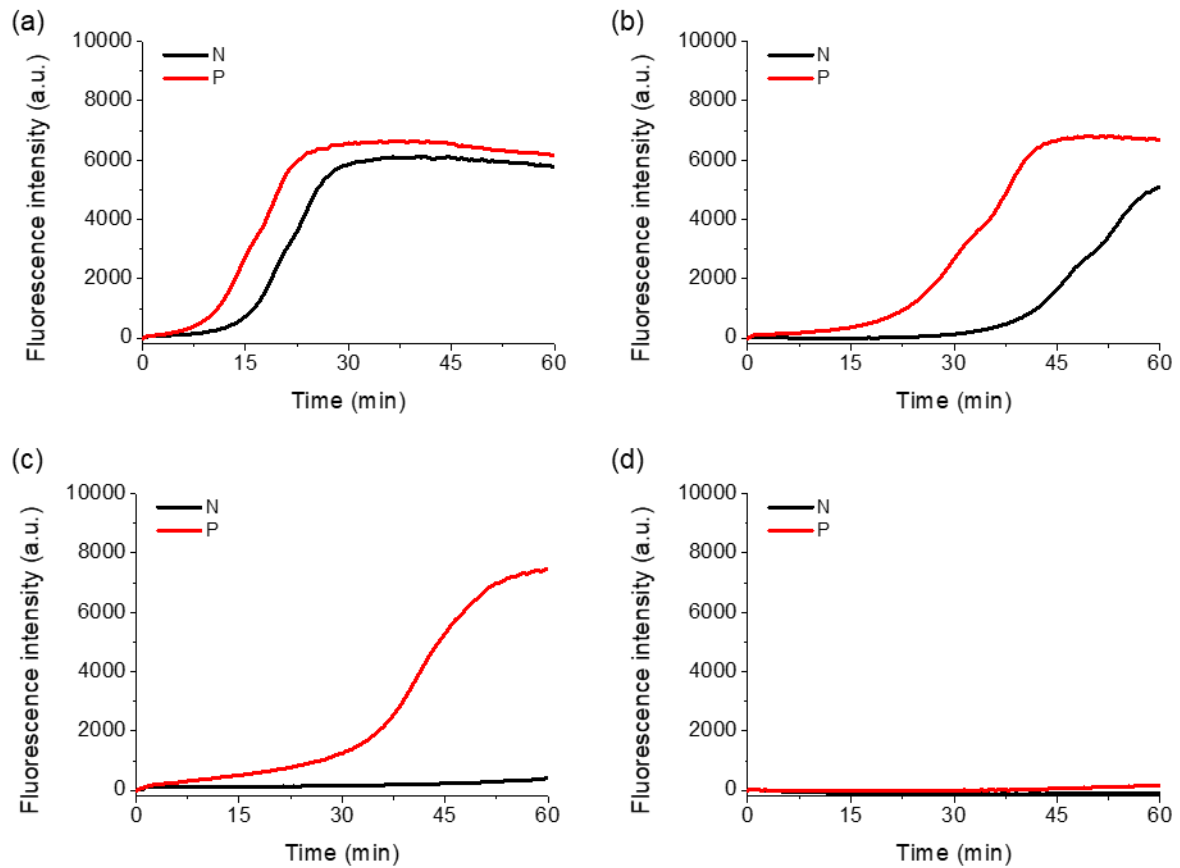


**Table S2.** Comparison of the MSH method with previous isothermal amplification methods for target RNA detection.

Key components/Methods	Detection limit	Limitations	Number of probes (primers)	Reference
Cascade Enzymatic Signal Amplification	1 fM	<ul style="list-style-type: none"> <li>• Labeling with fluorophore and quencher</li> <li>• Multiple primers</li> </ul>	5	S1
Primer generation-rolling circle amplification	~15 fM	<ul style="list-style-type: none"> <li>• Multiple reaction steps</li> </ul>	3	S2
Cleavage-mediated isothermal exponential amplification reaction	10 fM	<ul style="list-style-type: none"> <li>• Multiple reaction steps</li> <li>• High reaction temperature (55 °C)</li> </ul>	3	S3
Three-way junction-mediated amplification of G-quadruplex	1.23 pM	<ul style="list-style-type: none"> <li>• Low sensitivity</li> <li>• High reaction temperature (55 °C)</li> </ul>	2	S4
A hybridization-triggered DNAzyme cascade assay	1 pM	<ul style="list-style-type: none"> <li>• Labeling with fluorophore and quencher</li> </ul>	2	S5
Isothermal circular strand-displacement polymerization	6.4 fM	<ul style="list-style-type: none"> <li>• Labeling with fluorophore and quencher</li> <li>• Low sensitivity</li> </ul>	2	S6
G-quadruplex based two-stage isothermal amplification	2.5 pM	<ul style="list-style-type: none"> <li>• Short target RNA</li> <li>• Multiple reaction steps</li> </ul>	2	S7
Three-way junction-induced isothermal amplification	78.1 aM	<ul style="list-style-type: none"> <li>• High reaction temperature (55 °C)</li> </ul>	2	S8
Self-priming hairpins	28.9 aM	<ul style="list-style-type: none"> <li>• Design of two hairpin probes</li> </ul>	2	S9
Multifunctional self-priming hairpin	16.57 fM	-	1	This work

**Figure S10.** Specificity test of the MSH reaction with non-target RNAs exhibiting few mismatches. (a) The  $T_t$  values depending on the perfectly matched target RNA of different lengths; N60 and N20 represent a 60 nt or 20 nt-long RNA target, respectively. (b) The  $T_t$  values and the S.I. from the perfect matched and mismatched target RNAs. The  $T_t$  values are shown in the bar graph (left y-axis) and the S.I. values are plotted in the line graph (right y-axis). The final concentrations of target RNA, mismatched RNA, MSH probe, Nt.AlwI, and KF are 1 nM, 1 nM, 50 nM, 0.125 U/ $\mu$ L, and 0.2 U/ $\mu$ L, respectively.

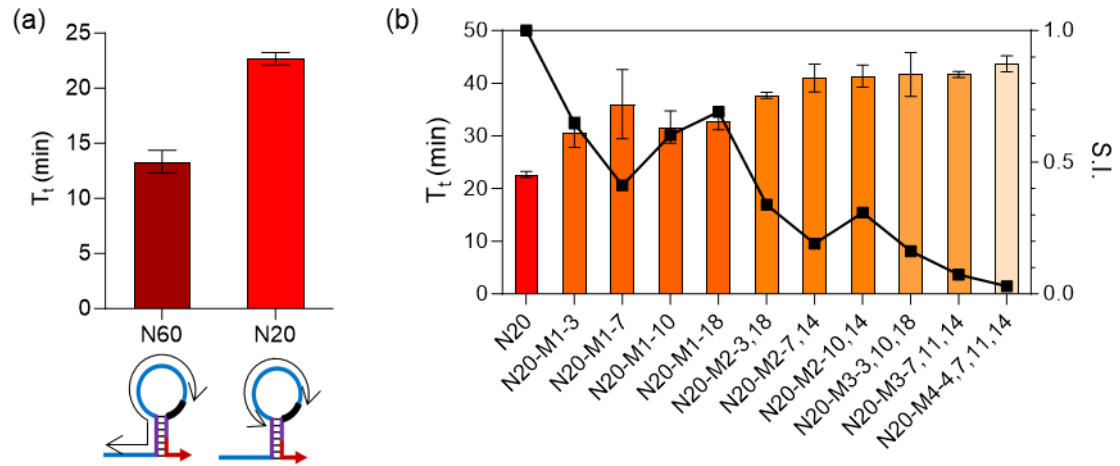


**Table S3.** Clinical sample test result by qRT-PCR and the MSH reaction.

Sample #	Sample type	qRT-PCR				MSH		
		C <sub>t</sub> (E)	C <sub>t</sub> (RdRp)	C <sub>t</sub> (N)	Diagnosis	45-T <sub>t</sub>	SD	Diagnosis
1	NPS	18.74	19.11	22.48	Positive	11.00	5.66	Positive
2	NPS	17.28	17.27	19.86	Positive	14.75	0.35	Positive
3	Sputum	29.60	30.34	29.16	Positive	8.00	0.71	Positive
4	NPS	31.94	32.36	35.61	Positive	11.75	6.01	Positive
5	Sputum	30.31	31.09	33.29	Positive	24.00	7.78	Positive
6	Sputum	25.98	26.08	31.33	Positive	10.75	4.60	Positive
7	Sputum	35.42	34.75	37.55	Positive	8.00	2.83	Positive
8	NPS	31.97	33.41	30.97	Positive	10.75	3.18	Positive
9	Sputum	31.09	31.54	34.45	Positive	11.00	1.41	Positive
10	Sputum	18.42	18.02	24.11	Positive	13.75	3.89	Positive
11	NPS	34.93	34.87	34.07	Positive	14.50	8.49	Positive
12	NPS	23.10	23.00	28.23	Positive	13.00	0.00	Positive
13	NPS	25.20	25.53	28.23	Positive	18.50	9.90	Positive
14	NPS	34.13	34.46	33.23	Positive	22.25	6.72	Positive
15	Sputum	19.46	19.86	19.08	Positive	12.00	2.12	Positive
16	Sputum	27.24	27.57	27.14	Positive	21.50	7.07	Positive
17	NPS	24.18	24.44	24.33	Positive	23.75	1.06	Positive
18	NPS	25.74	25.98	25.58	Positive	27.50	9.19	Positive
19	NPS	18.29	17.94	18.14	Positive	12.25	1.77	Positive
20	Sputum	19.35	19.04	19.44	Positive	19.00	14.14	Positive
21	Sputum	28.57	29.36	28.73	Positive	11.75	1.06	Positive
22	Sputum	16.93	16.70	17.89	Positive	19.25	4.60	Positive
23	Sputum	15.76	15.77	16.15	Positive	15.00	6.36	Positive
24	Sputum	26.98	26.84	27.32	Positive	11.50	2.83	Positive
25	Sputum	28.29	28.57	28.08	Positive	13.75	0.35	Positive
26	Sputum	24.88	24.52	24.98	Positive	16.50	0.00	Positive
27	NPS	34.13	35.27	33.22	Positive	0.00	0.00	Negative
28	NPS	34.33	35.87	33.62	Positive	0.75	1.06	Negative
29	Sputum	19.48	19.26	20.32	Positive	15.75	22.27	Positive
30	Sputum	26.46	26.86	27.29	Positive	9.50	5.66	Positive
31	NPS	N/A	N/A	N/A	Negative	0.50	0.71	Negative
32	NPS	N/A	N/A	N/A	Negative	2.00	1.41	Negative
33	NPS	N/A	N/A	N/A	Negative	0.00	0.00	Negative
34	NPS	N/A	N/A	N/A	Negative	1.75	2.47	Negative
35	NPS	N/A	N/A	N/A	Negative	1.25	1.77	Negative
36	NPS	N/A	N/A	N/A	Negative	2.00	2.83	Negative
37	NPS	N/A	N/A	N/A	Negative	2.50	3.54	Negative
38	NPS	N/A	N/A	N/A	Negative	0.00	0.00	Negative
39	NPS	N/A	N/A	N/A	Negative	0.50	0.71	Negative
40	NPS	N/A	N/A	N/A	Negative	0.00	0.00	Negative
41	NPS	N/A	N/A	N/A	Negative	0.75	1.06	Negative
42	NPS	N/A	N/A	N/A	Negative	1.25	1.77	Negative
43	NPS	N/A	N/A	N/A	Negative	0.00	0.00	Negative
44	NPS	N/A	N/A	N/A	Negative	0.00	0.00	Negative
45	NPS	N/A	N/A	N/A	Negative	0.00	0.00	Negative
46	NPS	N/A	N/A	N/A	Negative	0.00	0.00	Negative
47	NPS	N/A	N/A	N/A	Negative	0.00	0.00	Negative
48	NPS	N/A	N/A	N/A	Negative	5.50	7.78	Negative
49	NPS	N/A	N/A	N/A	Negative	5.25	7.42	Negative
50	NPS	N/A	N/A	N/A	Negative	2.50	2.83	Negative
51	NPS	N/A	N/A	N/A	Negative	0.50	0.71	Negative
52	NPS	N/A	N/A	N/A	Negative	6.00	8.49	Negative

53	NPS	N/A	N/A	N/A	Negative	0.00	0.00	Negative
54	NPS	N/A	N/A	N/A	Negative	4.75	6.72	Negative
55	NPS	N/A	N/A	N/A	Negative	5.25	7.42	Negative
56	NPS	N/A	N/A	N/A	Negative	4.25	6.01	Negative
57	NPS	N/A	N/A	N/A	Negative	4.75	6.72	Negative
58	NPS	N/A	N/A	N/A	Negative	5.25	7.42	Negative
59	NPS	N/A	N/A	N/A	Negative	6.00	4.95	Negative
60	NPS	N/A	N/A	N/A	Negative	9.75	1.77	Positive

## Reference (Supporting)

- S1. Wang, Huizhen, et al. "A hybridization-triggered DNzyme cascade assay for enzyme-free amplified fluorescence detection of nucleic acids." *Analyst* 144.1 (2019): 143-147.
- S2. Murakami, Taku, Jun Sumaoka, and Makoto Komiyama. "Sensitive RNA detection by combining three-way junction formation and primer generation-rolling circle amplification." *Nucleic acids research* 40.3 (2012): e22-e22.
- S3. Wang, Hui, et al. "Sensitive detection of mRNA by using specific cleavage-mediated isothermal exponential amplification reaction." *Sensors and Actuators B: Chemical* 252 (2017): 215-221.
- S4. Moon, Jeong, et al. "Urinary exosomal mRNA detection using novel isothermal gene amplification method based on three-way junction." *Biosensors and Bioelectronics* 167 (2020): 112474.
- S5. Zou, Bingjie, et al. "Ultrasensitive DNA detection by cascade enzymatic signal amplification based on Afu flap endonuclease coupled with nicking endonuclease." *Angewandte Chemie* 123.32 (2011): 7533-7536.
- S6. Guo, Qiuping, et al. "Sensitive fluorescence detection of nucleic acids based on isothermal circular strand-displacement polymerization reaction." *Nucleic acids research* 37.3 (2009): e20-e20.
- S7. Nie, Ji, et al. "G-quadruplex based two-stage isothermal exponential amplification reaction for label-free DNA colorimetric detection." *Biosensors and Bioelectronics* 56 (2014): 237-242.
- S8. Lee, Seoyoung, et al. "Three-way junction-induced isothermal amplification for nucleic acid detection." *Biosensors and Bioelectronics* 147 (2020): 111762.
- S9. Song, Ja Yeon, et al. "Self-priming hairpin-mediated isothermal amplification enabling ultrasensitive nucleic acid detection." *Analytical chemistry* 92.15 (2020): 10350-10356.